Relative intensities in the vibronic Zeeman effect in cubic crystals*

S. P. Pollack and R. A. Satten
Department of Physics, University of California, Los Angeles, California 90024
(Received 30 August 1972; revised manuscript received 15 October 1973)

Vibronic Zeeman intensity ratios are predicted for circularly polarized light propagation parallel to an externally applied magnetic field along [100] and [111] directions. A unique relative-intensity pattern is predicted for each type of site-symmetry vibration appearing in vibronic Zeeman patterns involving T_{1g} or T_{2g} electronic states. Experimental results in fields up to 62.8 kOe show semiquantitative agreement in most cases with predicted results for the ideal case of a limiting approximation in which T_{1u} and T_{2u}, etc., site-symmetry vibrations are not degenerate. Such degeneracy, rather than accidental, is typical of that required by the space-group symmetry of the crystal, and leads to departures from the limiting intensity ratios. Measurements of the departure from the limiting ratios can lead to the determination of the relative contribution of degenerate T_{1u}, T_{2u}, etc., site-symmetry vibrations. This information should provide quantitative data beyond that of zero-field vibronic intensity profiles in testing models for lattice-dynamics calculations applied to the vibronic interaction, or in evaluating necessary parameters of such models. Ideal π/σ vibronic intensity ratios for D_{3d} distortion of a cubic crystal field in zero magnetic field are also presented which explain certain observed polarizations not predicted by exact vibronic selection rules.

I. INTRODUCTION

With the advent of superconducting magnets it is possible to economically and conveniently achieve high fields which are sufficient to resolve the Zeeman effect of vibronic lines and bands. High fields are needed because vibronic lines often can be much broader than the parent zero-phonon lines of paramagnetic ions, such as rare earths and actinides, in crystals.

The peaks in vibronic bands are associated with peaks in the phonon density of states. Thus one studies such vibronic Zeeman transitions not only to infer g values of the parent electronic levels, but to learn about the phonons and their coupling to the bound electrons. However, the Zeeman splitting of vibronic bands gives no information about the phonons unless the relative density of phonon states is very large, as in the case of well-localized vibrations.[1] Thus, except for the latter, the Zeeman splitting of vibronic peaks in crystals is normally the same as the associated electronic levels. On the other hand, the relative intensity within a Zeeman pattern for a vibronic peak does reflect information about the phonons even when vibronic and parent electronic g values are equal.

In this paper we consider both theoretically and experimentally the problem of interpreting the relative intensity of circularly polarized electric dipole vibronic transitions for light propagating along the magnetic field [100] and [111] directions in cubic Cs_2UBr_6 and U^{4+} doped in cubic Cs_2ZrCl_6. The vibronic Zeeman spectrum in a cubic crystal is anisotropic in intensity, although isotropic in first-order level splitting; hence the understanding of an observed spectrum is greatly facilitated by an analysis of the theoretical intensities such as presented here. Calculated relative intensities are compared with experimental data for these crystals.

The calculated relative intensities are obtainable in a limiting approximation by group theory. The breakdown of this approximation can in principle be experimentally discovered by careful relative-intensity measurements and lead to information about lattice vibrations.

The theoretical intensity methods used here for cubic crystals are also applicable with further approximations to noncubic crystals in which there are atomic groupings such as the UCl_6^{2-} complex which have a symmetry distorted from octahedral. In this connection we report here a possible explanation for certain anomalous polarization results in the zero-field vibronic spectrum of trigonal Cs_2UCl_6. In this crystal the UCl_6^{2-} complex is at a site of D_{3d} symmetry. By treating the complex as octahedral with a D_{3d} distortion the latter plays a similar (although incomplete) role to the magnetic field in (partially) removing the degeneracies which would occur in purely octahedral symmetry. Earlier (unpublished) results[2] showed that certain vibronic lines relatively few in number had a polarization which could not be accounted for by exact vibronic selection rules involving phonons at any point in the Brillouin zone. The relative-intensity calculations presented here can account for such results; hence the approximations made presumably isolate the most important features of the problem. The missing σ polarizations, allowed by the exact selection rules in these cases, presumably occur only weakly.

II. CUBIC CASE

A. Theoretical intensities

We first examine what to expect theoretically for the relative intensities when the vibrations belong

to an irreducible representation of the site-symmetry group (O_h) of the U^{4+} site, as these relative intensities are determined entirely group theoretically. This involves an approximation which is discussed later in the paper. The electronic ground state[3] is nondegenerate A_{1g} and the only types of excited electronic states of Zeeman interest are either T_{1g} or T_{2g}, since other representations are either nondegenerate (A_{1g} and A_{2g}) or have no first-order Zeeman splitting (E_g). Essentially only $\Delta n = 1$ vibrational-quantum-number changes appear in the vibronic spectrum[4] and the vibronic splitting is the same as the parent electronic splitting.[1]

Circularly polarized light produces transitions from the singlet ground state to vibronic states belonging to particular rows of T_{1u}, which also are chosen to represent the reduced site symmetry in the magnetic field. The intensity of a circularly polarized vibronic transition from the A_{1g} ground vibronic state ψ_1 to an excited vibronic state ψ_2 is proportional to the absolute value squared of matrix elements of the form

$$\sum_j [a_j(\psi_2|V_{ev}|\psi_j)(\psi_j|\sum_i (x_i \pm iy_i)|\psi_1) + b_j(\psi_2|\sum_i (x_i \pm iy_i)|\psi_j)(\psi_j|V_{ev}|\psi_1)], \quad (1)$$

where the a_j and b_j contain appropriate energy denominators, and V_{ev} is the electron-phonon interaction which arises from the modulation of the crystalline field at the U^{4+} ion due to relative motion of the U^{4+} and surrounding ions. The circular polarization corresponding to the operator $\sigma_\pm = \sum(x_i \pm iy_i)$ is either called left handed (plus sign) or right handed (minus sign), using the convention that one observes the rotation sense of the $\vec{E}$ vector as the light approaches the observer. The ψ_k are first-order vibronic states and consist of products of electronic and vibrational wave functions, each of which and whose product belong to a row of the O_h site-symmetry irreducible representation, as well as forming one-dimensional representations of the lower symmetry group produced by the magnetic field H. For H along [100] the uranium-ion site symmetry is C_{4h} and for H along [111] the site symmetry is C_{3i}. Suitable vibronic basis functions for C_{4h} symmetry were given in Ref. 1 and, for C_{3i} are given in the Appendix of this paper.

In a strong magnetic field the Zeeman interaction lowers the symmetry by producing appreciable mixing of nondegenerate zero-field cubic wave functions. For the magnetic field along [111] there are no vibronic selection rules in a strong field involving T_{1u} or T_{2u} vibrations, assuming that the vibrational degeneracies are still not split by the magnetic field. Although our field attained 62.8 kOe, this must be regarded as a weak magnetic field for the purposes of intensity calculations, since the ratio of Zeeman splitting to energy separation between crystal-field levels is of the order of 10^{-2}. Thus the intensities of the vibronic Zeeman components are determined only by zero-order cubic wave functions. Nevertheless, the field is strong enough in many cases to fully resolve and separate these components.

The vibronic interaction V_{ev} is expanded in terms of site-symmetry coordinates $Q_i^{\alpha m}$ and, keeping only first-degree terms in Q, has the form

$$V_{ev} = \sum_{\alpha m i} f_i^{\alpha m} Q_i^{\alpha m}, \quad (2)$$

where $Q_i^{\alpha m}$ belong to the ith row of the α irreducible representation of the O_h site-symmetry group. The $Q_i^{\alpha m}$ are normalized linear combinations of displacements of symmetrically equivalent mth-nearest-neighbor atoms (or complexes) centered about a uranium site. The $Q_i^{\alpha m}$ in turn are proportional to normal coordinates of the lattice. Higher-degree terms in the Q are not needed for $\Delta n = \pm 1$ vibronic intensities.

Because the ground vibronic state transforms as A_{1g} and all cubic basis functions are uniquely determined by symmetry, the relative intensities of transitions to a particular vibronic Zeeman multiplet are given by symmetry-determined linear combinations of generalized (O_h group) Wigner coefficients which arise either in the square of a single matrix element of (1), such as

$$(\psi_2|V_{ev}|\psi_j), \quad (3)$$

where ψ_j transforms as either $x+iy$ or $x-iy$, or, in what gives the same result, the square of

$$(\psi_2|V_{ev}\sum(x_i \pm iy_i)|\psi_1). \quad (4)$$

The relations between matrix elements, such as given in the Appendix of Ref. 1, which are a consequence of the generalized Wigner-Eckhart theorem for cubic symmetry, are useful in obtaining the results. Since V_{ev} is an invariant under O_h operations, ψ_2 must also transform as $x \pm iy$. It is understood, of course, that x and y appearing in (1), (3), or (4) are orthogonal to the propagation direction, which is taken as the z axis. Although closure is sometimes employed in intensity calculations, because of the lack of knowledge of energy denominators, there is no need for the assumption of closure in the use of (3) or (4) to obtain relative intensities within a Zeeman multiplet; hence agreement with experiment of the calculated results in this paper is not a test of closure.

Interesting intensity-ratio patterns are predicted theoretically for right and left circularly polarized light in comparing propagation along [100] and [111] directions for the limiting cases in which the vi-

TABLE I. Relative intensities calculated for the three components of the vibronic Zeeman circularly polarized electric dipole transitions between an A_{1g} vibronic ground state and various vibronic levels involving T_{1g} and T_{2g} electronic states. Light propagation parallel to magnetic field directions along [100] and [111] are included. The allowed magnetic dipole zero-phonon transitions to T_{1g} levels are also shown. Relative intensities apply only within a vibronic multiplet, not between different multiplets. Different directions within a vibronic multiplet are comparable per paramagnetic ion.

		T_{1g} electronic states. Field direction		T_{2g} electronic states. Field direction	
Vibration	Polarization	[100]	[111]	[100]	[111]
T_{1u}	σ_+	110	110	022	114
	σ_-	011	011	220	411
T_{2u}	σ_+	022	114	110	110
	σ_-	220	411	011	011
E_u	σ_+	103	022	103	022
	σ_-	301	220	301	220
A_{2u}	σ_+	...	...	100	100
	σ_-	...	...	001	001
A_{1u} and zero phonon	σ_+	100	100	...	...
	σ_-	001	001	...	...

brational displacements transform according to an odd-parity irreducible representation of the site group about the paramagnetic ion. The calculated results summarized in Table I show that transitions to each odd-parity vibrational site-group irreducible representation coupled to a particular electronic state yield a unique intensity pattern when both propagation directions are considered.

Although most circularly polarized vibronic Zeeman intensity patterns are seen from Table I to be anisotropic, a simple argument demonstrates that the intensity pattern can be isotropic if both coupled electronic and vibrational states are angular momentum $J=1$ states, which form a basis for T_{1u}, since the Zeeman intensity pattern for coupled $J=1$ states does not depend on the direction of the magnetic field in space. This argument also makes it possible to conclude that for all propagation directions obtainable by operations of O_h acting on the [100] direction, the intensity pattern is the same if the excited electronic and vibrational states are both T_{1u}, even if not constructed of $J=1$ states. In particular, the pattern is the same for propagation along [110] for these states. However, the isotropy of the pattern for directions other than symmetry axes of the cube can only be expected to hold for $J=1$ states.

It is rather striking that densitometer traces of resolved vibronic Zeeman spectra, as shown in Figs. 1–3, exhibit relative-intensity patterns most of which are quite close to the limiting cases of Table I, but only T_{1u} and T_{2u} vibrations seem to appear. The latter probably reflects the fact that the nearest-neighbor interactions between the central ion and surrounding ligands are the most important for vibronic spectra and T_{1u} and T_{2u} are the only types of odd-parity symmetry displacements which an octahedral XY_6 complex can have, and possibly also the fact that the longest-range terms in the vibronic interaction involve T_{1u} modes.[5]

However, we do not wish to imply that this paper is concerned only with "internal" vibrations of the XY_6 complex, as much of our vibronic data comes from the "external" lattice bands. Further discussion of the expected intensity patterns is presented in Sec. IV.

B. Experimental results

It is helpful in discussing the experimental results to keep in mind the number of phonon

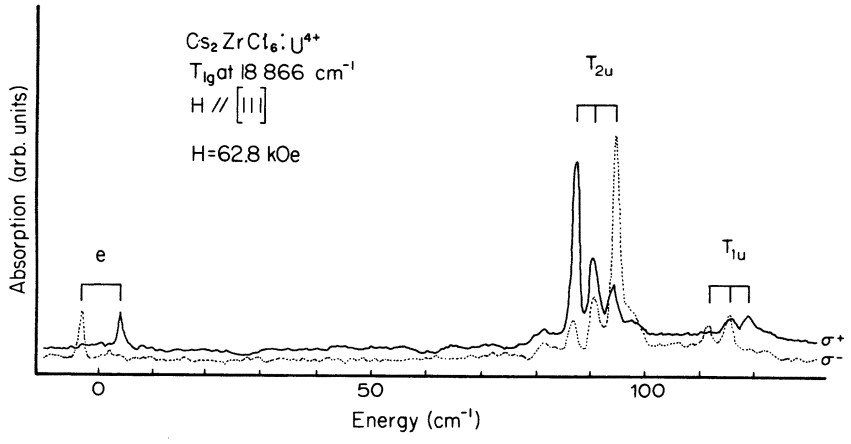

FIG. 1. Densitometer traces for right (dotted) and left (solid) circular polarization showing a portion of the Zeeman spectrum of $Cs_2ZrCl_6:U^{4+}$. Zero-phonon magnetic dipole transitions to the T_{1g} electronic level at 18 866 cm^{-1} are labeled e. The magnetic field $H=62.8$ kOe along [111]. In zero magnetic field the bracketed lines appear as a single line at the center of the bracket.

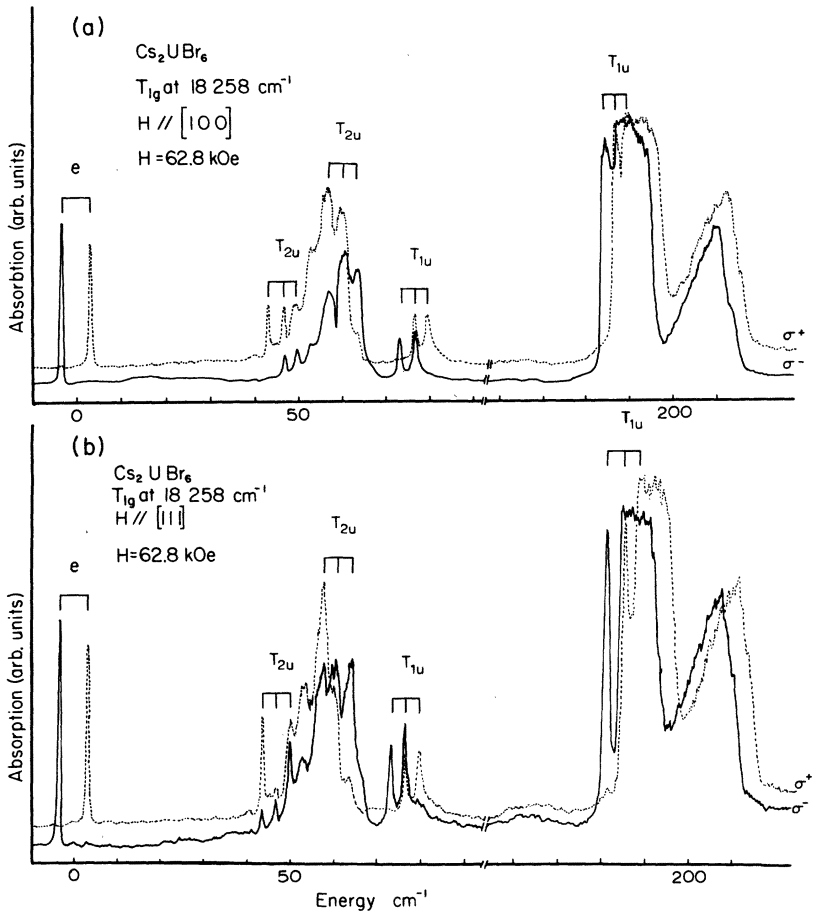

FIG. 2. Densitometer traces for right (solid) and left (dotted) circular polarization showing a portion of the Zeeman spectrum of Cs_2UBr_6. Zero-phonon magnetic dipole transitions to the T_{1g} electronic level at 18 258 cm^{-1} are labeled e. The magnetic field H = 62.8 kOe. (a) Propagation and field along [100]. (b) Propagation and field along [111]. In zero magnetic field the bracketed lines appear as a single line at the center of the bracket.

branches to expect for crystals such as Cs_2UBr_6 and Cs_2ZrCl_6, which have the O_h point-group and one molecule per primitive unit cell. Since we are not presenting phonon dispersion curves we shall for convenience enumerate only the phonons at the Γ point, although by this we do not wish to imply anything about the importance of $k=0$ phonons in the vibronic spectrum. The phonon branches at $k=0$ are Γ_1, Γ_{12}, Γ'_{15}, $2\Gamma'_{25}$, Γ_{25}, $3\Gamma_{15}$. The Γ_{25} and the two highest-energy Γ_{15} phonons have unit-cell vibrations concentrated largely in the T_{2u} and $2T_{1u}$, respectively, internal vibrations of the UBr_6^{2-} or UCl_6^{2-} complex.

The vibronic spectra of Cs_2UBr_6 and Cs_2ZrCl_6: U^{4+} crystals were obtained on photographic plates using a 2.5-m Ebert mounting spectrograph with a 4×5-in. grating having 600 lines/mm, and used in the fourth order. The figures presented here are densitometer traces of these plates. The Zeeman spectra were photographed with the crystals at 4.2°K using a superconducting magnet with field strengths up to 62.8 kOe. Circular polarization of the light was accomplished by a Glan-Thompson linear polarizer followed by a Fresnel rhomb.

Figure 1 shows a densitometer trace of a portion of the absorption spectrum of U^{4+} doped in Cs_2ZrCl_6 in left (σ_+) and right (σ_-) circular polarization in which the light propagation and field direction are along [111]. The upper electronic level is T_{1g} at 18 866 cm^{-1}. Only two magnetic dipole[6] zero-phonon Zeeman components (marked e) appear, since the middle line is forbidden. In the accompanying vibronic transitions only the internal vibrations appear. The crystal is too dilute with respect to U^{4+} ions to show the external vibrations in this as well as other absorption groups. Only the T_{2u} internal vibrations centered at 90 cm^{-1} and the T_{1u} internal vibrations at 115 cm^{-1} are shown in the figure, and they each clearly display relative-intensity patterns well approximated by the appropriate entries in Table I. The vibronic peak in the region 260–280 cm^{-1} associated with the other T_{1u} internal vibration of the UCl_6^{2-} complex is not shown because the Zeeman intensity pattern in the broad band is not resolved. Accurate relative-intensity measurements cannot be obtained from the densitometer traces of our photographic plates, so departures from the intensity ratios of Table I can-

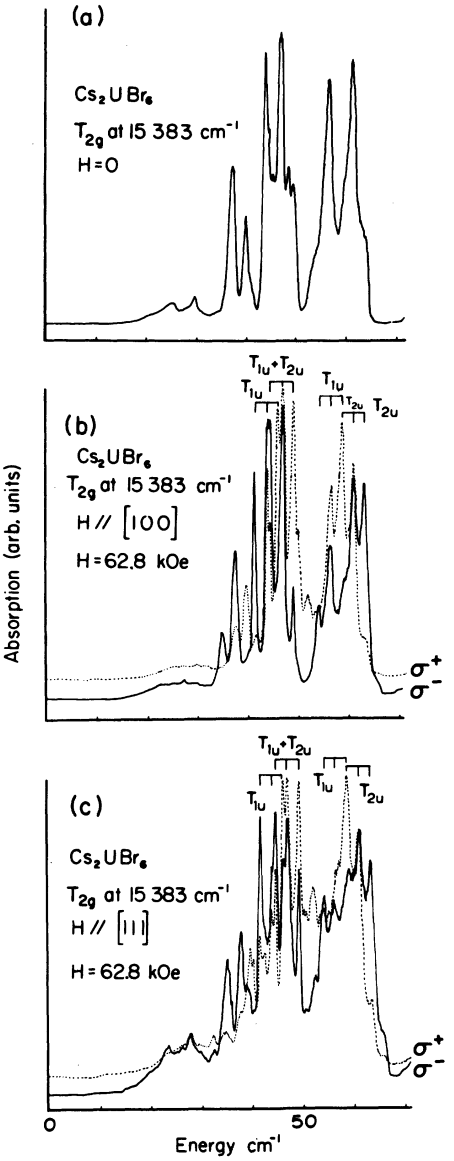

FIG. 3. (a) Densitometer trace of a portion of the vibronic spectrum of Cs_2UBr_6 associated with a transition to the T_{2g} electronic level at 15 383 cm^{-1} in zero field. (b) Densitometer traces for right (solid) and left (dotted) circular polarization for the same region as (a) but with $H = 62.8$ kOe along [100]. (c) Same as (b) but propagation and field along [111].

not be determined from our data.

The same T_{1g} electronic level in Cs_2UBr_6 is shifted to 18 258 cm^{-1}, and the vibrational frequencies are reduced largely owing to the increased mass from chlorine to bromine. Figure 2 shows the vibronic transitions associated with this electronic level. The difference in relative-intensity patterns between T_{1u} and T_{2u} vibrations in going from [100] to [111] directions is clearly shown by comparing Fig. 2(a) with Fig. 2(b). The lines centered at 47 and 61 cm^{-1} from the zero-phonon line are both clearly identifiable as T_{2u} vibrations, although there is only one Γ_{25} phonon. The line at 76 cm^{-1} follows a T_{1u} pattern and is due predominantly to the T_{1u} vibration of the UBr_6^{2-} complex corresponding to the 115-cm^{-1} vibration of UCl_6^{2-}. Although the Zeeman effect of the absorption bands centered at 186 and 210 cm^{-1} cannot be completely resolved, they are consistent with T_{1u} character. These bands correspond to the 260–280-cm^{-1} T_{1u} vibration of the UCl_6^{2-} complex split probably into TO and LO bands, the latter at the higher energy.

Figure 3(a) displays the considerable structure in the zero-field vibronic spectrum of Cs_2UBr_6 associated with the T_{2g} electronic level at 15 383 cm^{-1} in the region 35–65 cm^{-1}. The only predominantly internal vibration of the UBr_6^{2-} complex expected in this region is a T_{2u}, presumably the one at 61 cm^{-1}. The Zeeman effect of the four strongest vibronic lines in this region of the spectrum is presented in Figs. 3(b) and 3(c). In studying these figures one should realize that, owing to the small separation between some of the zero-field vibronic lines, some overlap of Zeeman patterns occurs. In particular, one component of the pattern centered at 56 cm^{-1} is located at the same energy as one of the components of the pattern centered at 61 cm^{-1}. The latter Zeeman pattern is that of a T_{2u} vibration just as in the case of the previously discussed electronic level. The peaks at 56 and 43 cm^{-1} follow reasonably well the pattern of a T_{1u} vibration. Although the vibration at 47 cm^{-1} exhibited a T_{2u} pattern in the vibronic spectrum coupled to the previously discussed T_{1g} electronic level, the pattern is not as clearly pure T_{2u} in the stronger absorption associated with the T_{2g} electronic level of Fig. 3. This pattern seems to be some combination of T_{1u} and T_{2u} and perhaps other vibration patterns, as is more clearly shown in the vibronic spectrum coupled to the T_{2g} electronic level at 12 612 cm^{-1} (Fig. 4), where the complication of overlapping Zeeman patterns is not present.

The presence of both T_{1u} and T_{2u} intensity contributions at a particular vibrational frequency can be confirmed by observing transitions from the ground A_{1g} to excited vibronic states involving A_{1g} and A_{2g} electronic levels. Selection rules permit transitions to A_{1g} electronic states coupled only to T_{1u} vibrations and transitions to A_{2g} electronic states coupled only to T_{2u} vibrations. To verify the existence of the same vibrational frequency appearing with more than one electronic level the energy of the upper electronic levels must be determined rather accurately indirectly, since both electric and magnetic dipole zero-phonon transitions are forbidden between A_{1g} and either A_{1g} or A_{2g} states. These energies can be determined by averaging the

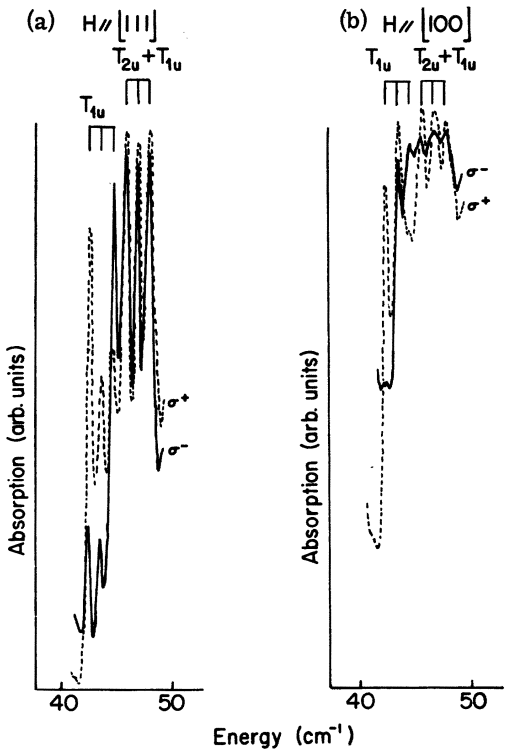

FIG. 4. Densitometer traces for right (solid) and left (dotted) circular polarization showing a portion of the vibronic Zeeman spectrum in the region 40–50 cm^{-1} above the T_{2g} level at 12 612 cm^{-1} in Cs_2UBr_6. The magnetic field $H = 62.8$ kOe. (a) Propagation and field along [111]. (b) Propagation and field along [100]. In zero magnetic field the bracketed lines appear as a single line at the center of the bracket.

frequencies of corresponding hot and cold bands at liquid-nitrogen temperature. Our field-free vibronic data for Cs_2UBr_6 involving previously identified[3] A_{1g} and A_{2g} electronic states have been particularly examined for the appearance of vibronic peaks corresponding to vibrational frequencies of 43, 47, 56, 61, and 76 cm^{-1}. The A_{1g} level at 14 692 cm^{-1} and the A_{2g} level at 11 796 cm^{-1} were used to form the following conclusions. The 43-cm^{-1} and 76-cm^{-1} lines appear coupled only to the A_{1g} electronic level, indicating T_{1u} vibrational character, and the line at 61 cm^{-1} appears coupled only to the A_{2g}, indicating a T_{2u} vibration. The vibrations at 47 and 56 cm^{-1} appear strongly in the vibronic spectrum coupled to both A_{1g} and A_{2g} electronic levels, indicating both T_{1u} and T_{2u} vibrations contribute at this frequency. However, in the Zeeman spectrum the 56-cm^{-1} line seems to fit the T_{1u} intensity pattern, although the departure from pure T_{1u} might have been masked by the proximity of the Zeeman pattern of the 61-cm^{-1} line.

The explanation, aside from accidental degeneracy, which accounts for departures from the intensity ratios of Table I is taken up in Sec. IV.

III. DISTORTED CUBIC CASE: TRIGONAL IN ZERO MAGNETIC FIELD

In trigonal crystals such as Cs_2UCl_2 the uranium atom is at a site of D_{3d} symmetry. The XY_6 complex is distorted from octahedral symmetry by compression along the [111] direction. We shall assume that the electronic and vibrational energy-level splittings appropriate to the reduction from octahedral to D_{3d} symmetry can be spectroscopically resolved. We lower the symmetry of the vibronic Hamiltonian but evaluate intensities with zero-order (cubic) electronic and vibrational wave functions.

The vibronic Hamiltonian for T_{1u} (octahedral) vibrations is then written

$$V_{\bullet v} = Af_1'q_1' + B(f_2'q_3' + f_3'q_2'), \tag{5}$$

where both the primed functions q_i' and f_i' are chosen so as to span both T_{1u} (octahedral) and one-dimensional C_3 representations as defined for q_i' in the Appendix. When $A = B$ in Eq. (5) then the latter becomes invariant under all operations of O_h, and can also then be written in the unprimed basis relative to fourfold axes as $V_{\bullet v} = A[f_1q_1 - f_3q_2 - f_2q_3]$, in which both the f_i and q_i transform as the q_i defined in the Appendix.

Similarly, the vibronic Hamiltonian for T_{2u} (octahedral) vibrations is written

$$V_{\bullet v} = aF_1'Q_1' + b(F_2'Q_3' + F_3'Q_2'), \tag{6}$$

where both the primed functions Q_i' and F_i' are chosen to span both T_{2u} (octahedral) and one-dimensional C_3 representations as defined for Q_u' in the Appendix. When $a = b$ in Eq. (6) then the latter becomes invariant under all operations of O_h and can also be written in the unprimed basis relative to fourfold axes as $V_{\bullet v} = a(F_1Q_1 + F_2Q_3 + F_3Q_2)$, in which both the F_i and Q_i transform as the Q_i defined in the Appendix.

The relative intensities in zero magnetic field of π and σ (E vector parallel and perpendicular, respectively, to the threefold axis) electric dipole transitions connecting the A_{1g} ground state with the various possible vibronic states formed from all possible electronic states coupled with the split components of T_{1u} vibrational states are shown in Table II. In reading Table II only intensity ratios should be formed from entries which refer to electronic and vibrational states respectively degenerate in octahedral symmetry. The various ratios thereby obtained are independent of electronic state since the electronic matrix elements cancel out. Note that when $A = B$ the ratio of π to σ intensities equals unity if all contributions split from a particular octahedral electronic and vibrational level are

TABLE II. Relative intensities of vibronic transitions for D_{3d} distortion of cubic symmetry. [Ratios are to be formed involving electronic and vibrational states respectively degenerate in octahedral symmetry. The various ratios thereby obtained are independent of electronic state since the electronic matrix elements cancel out. The A/B ratio is the same as for V_{ev} of Eq. (5).]

Electronic states		Octahedral T_{1u} vibrational states in D_{3d} field		
O_h	D_{3d}	Polarization	$A_{2u}(D_{3d})$	$E_u(D_{3d})$
A_{1g}	A_{1g}	π	A^2	...
		σ	...	B^2
A_{2g}	A_{2g}	...	...	...
E_g	E_g	π	...	$2B^2$
		σ	A^2	B^2
T_{1g}	A_{2g}	π	...	...
		σ	...	B^2
	E_g	π	...	$2B^2$
		σ	A^2	...
T_{2g}	A_{1g}	π	$4A^2$	...
		σ	...	B^2
	E_g	π	...	$2B^2$
		σ	A^2	$4B^2$

added together for each polarization, in agreement with what is expected for the strictly octahedral case.

Table II also shows the possibility of a pure-π-only transition from the A_{1g} ground state to a vibronic level in which the electronic state is $E_g(D_{3d})$ arising from $T_{1g}(O_h)$. Although such lines have been observed experimentally,[2] they could not be understood on the basis of exact selection rules for vibronic transitions involving phonons at various points in the Brillouin zone. In particular, there are no predicted π-only transitions from a ground A_{1g} state to an excited $E_g(D_{3d})$ electronic level coupled to a phonon, according to exact selection rules,[2,7,8] regardless of where in the Brillouin zone the phonon comes from. Although exact selection rules should be obeyed in predictions about forbidden transitions, it is well known that transitions *not* forbidden by exact selection rules may have other reasons for appearing only weakly or not at all. Such is the situation here in exact analogy to the difference between the strong- (magnetic) field and weak-field case discussed earlier for cubic symmetry. The D_{3d} symmetry component of the crystal field is small compared to the octahedral component, as judged by its relative effect in splitting the energy levels. The ratio of D_{3d} to octahedral splitting is of the order of 10^{-1}, so only small mixing of octahedral wave functions results.

In a like manner Table III shows results for the relative intensities in zero magnetic field of π and σ electric dipole transitions connecting the A_{1g} ground state with the various possible vibronic states formed from all possible electronic states coupled with the split components of T_{2u} vibrational states. As in Table II, only intensity ratios should be formed which refer to electronic and vibrational states respectively degenerate in octahedral symmetry. Similar comments concerning Table III can be made as for Table II.

It should be emphasized that the intensity ratios obtainable from Tables II and III depend not only on the use of zero-order cubic wave functions for D_{3d} symmetry, but are also subject to the limiting approximation of this paper, which also holds for cubic crystals, and which is discussed in Sec. IV on lattice-dynamics considerations.

IV. LATTICE-DYNAMICS CONSIDERATIONS: LIMITING APPROXIMATION

It is well known that the vibrational modes of a molecule belong to an irreducible representation of the point group of the molecule. Barring accidental degeneracies each eigenfrequency is associated with its own irreducible representation.

If a crystal is treated as a very large molecule, the vibrational modes can also be classified according to irreducible representations of the point group appropriate to a particular site. It seems to be not always appreciated that in such a description, except for $k = 0$ and a few special cases, normal modes belonging to various *differ-*

TABLE III. Relative intensities of vibronic transitions for D_{3d} distortion of cubic symmetry. [Ratios are to be formed involving only electronic and vibrational states respectively degenerate in octahedral symmetry. The various ratios thereby obtained are independent of electronic state since the electronic matrix elements cancel out. The a/b ratio is the same as for V_{ev} of Eq. (6).]

Electronic states		Octahedral T_{2u} vibrational states in D_{3d} fields		
O_h	D_{3d}	Polarization	$A_{1u}(D_{3d})$	$E_u(D_{3d})$
A_{1g}	A_{1g}	...	...	...
A_{2g}	A_{2g}	π	a^2	...
			...	b^2
E_g	E_g	π	...	$2b^2$
		σ	a^2	b^2
T_{1g}	A_{2g}	π	$4a^2$	...
		σ	...	b^2
	E_g	π	...	$2b^2$
		σ	b^2	$4b^2$
T_{2g}	A_{1g}	π	...	...
		σ	...	b^2
	E_g	π	...	$2b^2$
		σ	a^2	...

ent irreducible representations of the site group must be degenerate. This is a consequence of the space-group symmetry of the crystal. The occurrence of such a degeneracy is clearly important for the calculation of vibronic intensities, as the intensity ratios of Table I depend on the existence of only one dominant site-symmetry vibrational irreducible representation for a given vibronic peak.

Although there is more than one way to demonstrate the above degeneracy, one general proof is as follows: In the conventional description normal coordinates of a crystal are described in terms of plane waves. Those modes having a particular wave vector $\vec{k}$ and transforming according to some irreducible representation of the group of the $\vec{k}$ vector, will, together with all other degenerate modes belonging to the remaining symmetrically equivalent $\vec{k}$ vectors of the star, form a basis for an irreducible representation of the space group. The latter is reducible as a representation of a site group. The site-group irreducible representations contained in the space-group irreducible representation provide alternate descriptions of degenerate normal modes of the crystal. The various site-group modes (not to be confused with local modes) thus contained, although belonging to different irreducible representations of the site group, are clearly degenerate as they are linear combinations of the degenerate wave modes which were bases for the original space-group representation. Such decompositions have been presented for the space group O_h^5 by Loudon[8] and for C_{6h}^2 by Satten.[7] For example, from the table given by Loudon[8] for O_h^5 it is evident that for all but a few exceptional points in the Brillouin zone there will be degenerate T_{1u} and T_{2u} modes in a site-group description for O_h symmetry sites. For a general point in the Brillouin zone, in which the point group of the $\vec{k}$ vector consists of the identity alone, the space-group representation contains each O_h site-group representation as often as its dimensionality.[9]

These considerations lead us to expect departures from the intensity ratios of Table I, particularly for the external lattice vibrations, and we have cited some examples occurring in the spectrum of Cs_2UBr_6. Such departures are accounted for by abandoning the limiting approximation of a single dominant site-symmetry vibrational irreducible representation, and instead including all those which are contained in the space-group representation and allowed by selection rules. Since only odd-parity vibrations affect the intensity it follows that the intensity of each vibronic peak can be expressed as a linear combination of at most four parameters, one parameter for each allowed odd-parity irreducible representation of O_h. This reduces to three parameters if one neglects the necessarily small A_{1u} vibrational contribution, which in principle appears for vibronic transitions to T_{1g} electronic levels. A_{1u} site-symmetry vibrations are unlikely to appear in the f^n configuration vibronic spectrum[10] because they would involve spherical harmonics $Y_{l,m}$ of degree $l=9$ or higher in electron coordinates in V_{ev}, and besides cannot occur except for atoms beyond second nearest neighbors to the uranium atom.

For a vibronic peak associated with a T_{2g} electronic level, suppose the intensity of the T_{1u}, T_{2u}, E_u, A_{2u} site-symmetry vibrations each acting alone without the others would have produced, respectively, the intensities a, b, c, d times the corresponding intensities in Table I. Then the actual intensity ratio R_1 of one outer line to the central line of a three-line Zeeman pattern for propagation along [100] is given by

$$R_1=\frac{2a+3c}{2a+b}. \tag{7}$$

The appropriate one of the two outer spectral lines must be used for Eq. (7) to apply. For the other outer line in the same circular polarization the similar ratio to the central line is

$$R_2=\frac{b+c+d}{2a+b}. \tag{8}$$

Along [111] we obtain the corresponding intensity ratios of an outer to the central Zeeman component:

$$R_3=\frac{4a+2c}{a+b+2c} \tag{9}$$

and

$$R_4=\frac{a+b+d}{a+b+2c}. \tag{10}$$

Three of the equations (7)–(10) can be solved for three parameter ratios b/a, c/a, d/a if $a\neq 0$. In the latter case the parameter ratios a/b, c/b, d/b can be solved for. The fourth equation leads to a connection between the intensity ratios R_1, R_2, R_3, R_4. From the way in which the intensity ratios R_i are constructed they obviously reduce to the ratios of simple integers given by Table I when all but one of the a, b, c, d are zero.

For vibronic transitions involving a T_{1g} electronic level, if one ignores the A_{1u} vibrations and introduces the analogous intensity parameters A, B, C, one obtains in an analogous way after solving the equations the result

$$\frac{C}{A}=\frac{R_1+R_2-1}{1+3R_1-R_2} \tag{11}$$

and

$$\frac{B}{A}=\frac{3-3R_1+R_2}{2(1+3R_1-R_2)}, \tag{12}$$

where R_1 and R_2 are similarly defined ratios for the [100] propagation direction. The [111] direction introduces a ratio R_3 which connects R_1 and R_2.

The experimental determination of these vibronic-intensity-parameter ratios should provide additional quantitative information for lattice-dynamics calculations based on optical data, and for the vibronic interaction not thus far obtained from vibronic spectra. This information goes beyond that obtainable from intensity profiles of zero-field vibronic bands by separating the contributions to each vibronic peak into significant parts. It is hoped that the experimentally determined intensity-parameter ratios will, together with other optical data, assist in the determination of the large number of parameters required by the more sophisticated lattice-dynamics models.[10-13]

Having accounted in principle for departures from the limiting ratios of Table I, the question becomes why are the intensity ratios of Table I so nearly followed in many vibronic peaks. There is probably no single reason applicable to all vibronic peaks. In the following we discuss the situation.

We do not expect departures from the intensity ratios of Table I to be due to phonons near $k=0$. The reason can be most simply understood in terms of an example. Consider degenerate Γ_{25} phonons. The vibrations of the XY_6 complex transform as T_{2u}. For degenerate phonons from the same branch having $\vec{k}$ vectors very close to $k=0$, a symmetrically equivalent "shell" of XY_6 complexes under operations relative to the central-cell origin will have vibrational amplitudes which are much larger for T_{2u} than any other type of vibration, as long as the distance to the shell from the origin is much smaller than the phonon wavelength. When k is small one must go so far from the central cell to build up other amplitudes than T_{2u} for the shell that the vibronic interaction between shell and central ion would be negligible.

For phonon branches which involve mainly the internal vibrations of the XY_6 complex the relative-intensity pattern is easiest to understand. These peaks seem to involve fairly pure T_{1u} or T_{2u} vibrations. Owing in part to the relatively large amplitude of vibration concentrated in the complex for such modes, the nearest-neighbor vibronic interactions no doubt dominate the vibronic intensity mechanisms. The entire complex is within a primitive unit cell and the only odd-parity O_h symmetry coordinates of an XY_6 complex which can be formed transform as T_{1u} or T_{2u}. Even though unit-cell eigenvectors of the dynamical matrix[14] for $k\neq 0$ are linear combinations of those at $k=0$, it is reasonable to expect that for phonon branches in which internal vibrations predominate, the amplitude of the T_{1u} or T_{2u} symmetry coordinates in the unit-cell motion will not both be relatively large in a particular optical branch, but at most only one or the other type dominate throughout most of the Brillouin zone. For example, the phonon branch which is Γ_{25} at $k=0$ will have a unit-cell eigenvector with the largest amplitude concentrated in the T_{2u} motion of the XY_6 complex throughout most of the Brillouin zone. This was found to be the case in the lattice-dynamics calculation for Cs_2UBr_6 of Chodos.[10,11]

For phonon branches which involve mainly external vibrations the relative amplitudes in the unit-cell eigenvectors cannot be expected to have a dominant symmetry coordinate throughout the Brillouin zone; hence the unit-cell eigenvectors and the density of states must be determined from a lattice-dynamics calculation. For crystals such as Cs_2UBr_6 and Cs_2ZrCl_6 having O_h^5 space groups, site-symmetry vibrations involving the cesium atoms in particular can be expected to be of importance since they are second nearest neighbors to the central X atom of the XY_6 complex. There are two cesium atoms per primitive unit cell, but eight symmetrically equivalent cesium atoms comprising the second-nearest-neighbor shell. The three Cartesian components for each of the eight cesium atoms form the basis of a reducible representation which factors into $A_{1g}+A_{2u}+E_g+E_u+T_{1g}+2T_{1u}+2T_{2g}+T_{2u}$ site-symmetry irreducible representations. Which of these types of site-symmetry motions occurs for degenerate phonons of any particular type in the conventional wave description is obtainable from the decomposition table of Loudon.[8] Their amplitudes for such phonons are obtainable from the unit-cell eigenvectors. T_{1u} or T_{2u} site-symmetry vibrations of the eight nearest cesiums to the central uranium atom will be accompanied by T_{1u} or T_{2u} motions respectively of the XY_6 complex. Unless the latter amplitudes are very small relative to the cesiums they may also contribute to the vibronic intensity owing to their greater proximity to the central atom. If E_u vibrations contribute to vibronic transitions to T_{1g} or T_{2g} electronic states they must be due to cesium vibrations or beyond. The E_u vibrations are forbidden by selection rules to be observable in vibronic transitions to A_{1g}, A_{2g}, or E_g electronic states from the ground A_{1g}. The presence of E_u site-symmetry vibrations in the vibronic spectrum can only be determined experimentally by measuring the departure of the vibronic intensity ratios from the limiting ratios of Table I and solving for c/a or c/b intensity ratios, as discussed above, since no intensity pattern resembling the pure-E_u case of Table I was observed in the spectrum.

Departures from the intensity ratios of Table I will not occur for certain phonon peaks for group-theoretic reasons. Thus there are phonons in the Brillouin zone for which T_{1u} site-symmetry vibra-

tions occur without any other odd-parity vibrations, and similarly for T_{2u}. Besides the obvious Γ-point phonons, it can be seen from Loudon's table[8] of site-group representations contained in the O_h^5 space-group representations that the following special types of phonons (together with those degenerate in the star) have T_{2u} site-symmetry vibrations surrounding the uranium site without any other odd-parity vibrations: X_3', W_1, Δ_2. To this list should be added L_1' and Λ_2 phonons, which yield A_{1u} vibrations as well, and Σ_2 phonons, which produce both A_{1u} and E_u vibrations in addition to T_{2u}, but no T_{1u}. However, A_{1u} site-symmetry vibrations are unlikely to appear in the vibronic spectrum, as already mentioned. Similarly, the phonons in the star of X_4', W_2', Δ_1 have T_{1u} site-symmetry vibrations without any other odd-parity vibrations, L_2' and Λ_1 have T_{1u} and A_{2u}, and Σ_3 yields T_{1u}, A_{2u}, and E_u, but all have T_{1u} without T_{2u}.

It is, of course, understood that a single phonon would not be observed in the vibronic spectrum. However, it is reasonable to expect phonons contributing to a vibronic peak to have eigenvectors which do not vary much over the peak. Hence, if one of the above special phonons were included in the peak, one would expect all the phonons contributing to the peak to produce site-symmetry vibrations in which T_{1u} and T_{2u} vibrations are negligible.

Although such special phonons exist, which do not produce both T_{1u} and T_{2u} site-symmetry vibrations, we are not suggesting this as a universal explanation for those cases in which there is agreement with the relative intensities of Table I. We can be fairly certain that what is forbidden by group theory will not appear. But, as we have seen, we cannot always expect that what is allowed will appear.

APPENDIX

The following define basis functions for the octahedral group O which are also bases for one-dimensional representations for C_3. It is worth noting that these C_3 basis functions are also bases for D_3, which accounts for some of the zeros in Tables I, II, and III.

$T_{1u}(0)$:

$$A_1(C_3): \quad q_1' = (3)^{-1/2}[q_1 - q_2(1-i)/\sqrt{2} + q_3(1+i)/\sqrt{2}],$$

$$E_1(C_3): \quad q_2' = (3)^{-1/2}[q_1 + q_2(\sqrt{3}+1)(1-i)/2\sqrt{2} + q_3(\sqrt{3}-1)(1+i)/2\sqrt{2}],$$

$$E_2(C_3): \quad q_3' = (3)^{-1/2}[q_1 - q_2(\sqrt{3}-1)(1-i)/2\sqrt{2} - q_3(\sqrt{3}+1)(1+i)/2\sqrt{2}],$$

where q_1, q_2, q_3 transform like z, $-(x+iy)/\sqrt{2}$, $(x-iy)/\sqrt{2}$, respectively, under operations of O with x, y, z along four-fold axes. Then q_1', iq_2', iq_3' transform like z', $-(x'+iy')/\sqrt{2}$, $(x'-iy')/\sqrt{2}$, respectively, where $z' = \vec{r}\cdot(\vec{i}+\vec{j}+\vec{k})/\sqrt{3}$, $x' = \vec{r}\cdot(\vec{i}-\vec{j})/\sqrt{2}$, $y' = \vec{r}\cdot(\vec{i}+\vec{j}-2\vec{k})/\sqrt{6}$, in which $\vec{i}$, $\vec{j}$, $\vec{k}$ are unit vectors along the four-fold axes.

$T_{2u}(0)$:

$$A_1(C_3): \quad Q_1' = (3)^{-1/2}[Q_1 - Q_2(1+i)/\sqrt{2} - Q_3(1-i)/\sqrt{2}],$$

$$E_1(C_3): \quad Q_2' = (3)^{-1/2}[Q_1 - Q_2(\sqrt{3}-1)(1+i)/2\sqrt{2} + Q_3(\sqrt{3}+1)(1-i)/2\sqrt{2}],$$

$$E_2(C_3): \quad Q_3' = (3)^{-1/2}[Q_1 + Q_3(\sqrt{3}+1)(1+i)/2\sqrt{2} - Q_3(\sqrt{3}-1)(1-i)/2\sqrt{2}],$$

where Q_1, Q_2, Q_3 transform like $2^{-1/2}(Y_{2,2} - Y_{2,-2})$, $Y_{2,1}$, $Y_{2,-1}$, respectively.

---

*Work supported in part by the U. S. Army Research Office (Durham).

[1]R. A. Satten, D. R. Johnston, and E. Y. Young, Phys. Rev. 171, 370 (1968).
[2]D. R. Johnston, Ph.D. dissertation (University of California, Los Angeles, 1967) (unpublished).
[3]D. R. Johnston, R. A. Satten, C. L. Schreiber, and E. Y. Wong, J. Chem. Phys. 44, 3141 (1966).
[4]R. A. Satten, C. L. Schreiber, and E. Y. Wong, J. Chem. Phys. 42, 162 (1965).
[5]T. Timusk and M. Buchanan, Phys. Rev. 164, 345 (1967).
[6]D. Johnston, R. Satten, and E. Wong, J. Chem. Phys. 44, 687 (1966).
[7]R. A. Satten, J. Chem. Phys. 40, 1200 (1964).
[8]R. Loudon, Proc. Phys. Soc. Lond. 84, 379 (1964).
[9]S. A. Pollack and R. A. Satten, J. Chem. Phys. 36, 804 (1962).
[10]S. Chodos, Ph.D. dissertation (University of California, Los Angeles, 1971) (unpublished).
[11]S. Chodos, J. Chem. Phys. 57, 2712 (1972).
[12]G. P. O'Leary and R. G. Wheeler, Phys. Rev. B 1, 4409 (1970).
[13]W. E. Bron, Phys. Rev. 185, 1163 (1969).
[14]A. A. Maradudin, E. W. Montroll, and G. H. Weiss, in *Solid State Physics*, edited by F. Seitz and D. Turnbull (Academic, New York, 1963), Suppl. 3.